

Design analysis of Tesla micro-turbine operating on a low-boiling medium

Piotr Lampart, Krzysztof Kosowski,
Marian Piwowarski, Łukasz Jędrzejewski

Abstract

This paper presents results of the design analysis of a Tesla bladeless turbine intended for a co-generating micro-power plant of heat capacity 20 kW, which operates in an organic Rankine cycle on a low-boiling medium. Numerical calculations of flow in several Tesla turbine models were performed for a range of design parameters. Results of investigations exhibit interesting features in the distribution of flow parameters within the turbine interdisk space. The calculated flow efficiency of the investigated Tesla turbine models show that the best obtained solutions can be competitive as compared with classical small bladed turbines.

Keywords: Tesla turbine, axial flow bladed turbine, flow efficiency, CFD calculations, RANS model

Introduction

It is a rather common opinion that bladed turbines are unbeatable as compared with Tesla turbines in the range of large power outputs. However, at very small outputs some superiority of bladeless turbines can be expected, Fig. 1. In a majority of published cases, rotational speeds of Tesla turbine rotors appear lower than those of bladed turbines, which makes the selection of an electric generator easier.

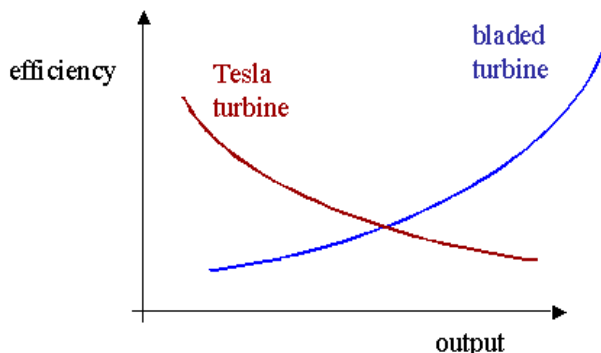


Fig. 1 Pictorial comparison of efficiency of small bladed and Tesla turbines

The first bladeless turbine was designed and manufactured by Nikola Tesla (in 1913) [11]. The design makes use of the effects which occur in the boundary layer flow between the rotating disks placed very close to one another (Fig. 2). The gas flowing spirally from the outer to inner part transfers energy to the rotating disks. The supply usually takes place from several nozzles discretely located along the circumference. The medium flows out through the holes in the disks situated near the turbine shaft.

Distances between disks are very small. The highest value of efficiency appears when they are approximately equal to the double boundary layer thickness [9]. The efficiency of the Tesla turbine depends on many parameters, namely on: pressure, temperature, inlet medium velocity, number, diameter, thickness and distance between the disks as well as on the state of the disk surface, rotational speed of the rotor, flow kinematics at the inlet to and outlet from the turbine, etc. In the subject-matter literature, examples of experimental research referring to the following models of Tesla micro-turbines can be found:

- ~3.0kW output power, 15000 rpm, 32% efficiency, [5];
- ~1.0kW output power, 12000 rpm, 24% efficiency, [1];
- ~1.5kW output power, 12000 rpm, 23% efficiency, [8, 9];
- ~50W output power, 1000 rpm, 21% efficiency, [7];
- ~1.5kW output power, 12000 rpm, 49% efficiency, [3].

Experimental works aimed first of all at establishing relationships between the turbine efficiency and parameters given below:

- distance between the micro-turbine disks;
- number and diameter of the micro-turbine disks;
- number of inlet nozzles to the micro-turbine;
- rotational speed of the rotor;
- medium inlet pressure;

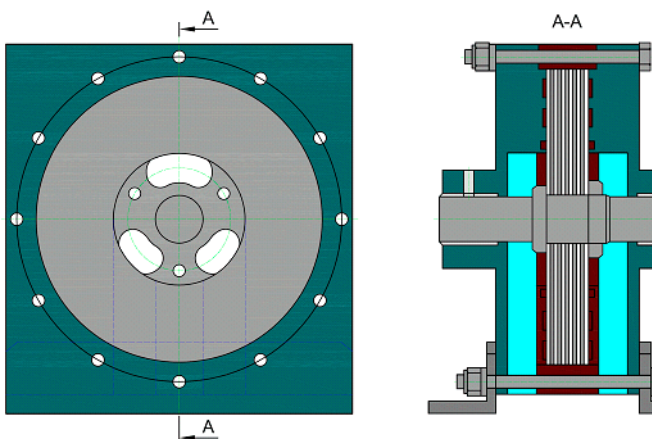


Fig. 2 Tesla turbine [11]

- medium inlet temperature;
- medium inlet velocity and inlet angle;
- corrosion and erosion of micro-turbine elements;
- constructional materials (composites, ceramic materials, bronzes, aluminium alloys);
- kind of medium flowing through the micro-turbine (air, biogas, organic agents, exhaust gases, multi-phase media, etc).

Main design features and operational parameters of Tesla turbines published in the literature referenced in this paper are presented in Tab. 1. Not only turbines but also compressors, pumps and gas turbine sets can be built on the basis of the same working principle.

Preliminary design analysis

CFD calculations of various models of Tesla disk turbines were carried out on the basis of the RANS model supplemented by the $k-\omega$ SST turbulence model available in the computer programme Fluent [12]. Numerical discretisation of the set of fundamental

equations is performed using the finite volume method. The “segregated” solver with the sequential solving of the governing equations as well as the SIMPLE algorithm for correction of pressure and velocity are applied. Discretisation of convection fluxes is performed using an “upwind” scheme of the 2nd order accuracy. The time-domain discretisation is made by an “implicit” scheme. The calculations are carried out until the stationary state is reached, lowering the residua of particular equations by 4÷6 orders of magnitude.

The calculation domain was prepared by means of the software Gambit [14]. The models of Tesla turbines contain the inlet nozzle, a half of the single interdisk space (under the assumption on flow symmetry in a central plane) as well as the outlet area. The models analyzed in this work represent a simplification of real geometry of Tesla turbines. The outlet area was simplified in a way to allow the medium outflow from the turbine flow passage along the entire circumference of the shaft. The presence of the tip clearance was neglected. The calculations were carried out in a fixed (motionless) reference frame, with turbine disk walls kept in rotational motion. In accordance with the assumed turbulence model, the calculation grid

Tab. 1. Specification of Tesla turbine design solutions

No	Outer diam. of disk	Disk thickness	Interdisk distance	Inner diam. of disk	Number of disks	Rotational speed	Moment	Power	Medium	Inlet pressure	Inlet temperature	Nozzle diameter	Nozzle surface area	Nozzle angle	Efficiency
	D_1	t	b	D_2	z	n	T	N		p_0	t	D	S	α	η
	[m]	[m]	[m]	[m]	[-]	[rpm]	[Nm]	[kW]		[kPa]	[°C]	[m]	[mm ²]	[°]	[-]
1	-	-	-	-	6	18000	-	2,983	Air	615,29	-	-	-	-	0,35
2	-	-	-	-	-	8193	-	8,650	Air	593,00	-	-	-	-	-
3	0,17780	0,0024	0,0016	-	7	10000	-	-	Air	861,84	-	-	-	15	0,232
4	0,17780	0,0024	0,001	-	11	9200	-	-	Air	377,14	-	-	-	10	0,258
5	0,20320	0,0005	0,0005	0,0335	24	17000	-	-	Air	615,29	-	-	-	20	0,35
6	0,30480	0,0008	0,0008	0,07620	45	1100	-	0,447	Air	227,53	20,5	-	121	15	0,16
7	0,30480	0,0008	0,0008	0,07620	45	6218	-	3,430	Gas	275,79	444	-	-	15	0,123
8	0,30480	0,0008	0,0008	0,07620	45	6284	-	3,206	Biomass	275,79	391,6	-	-	15	0,11
9	0,30480	0,0008	0,0008	0,07620	45	6500	-	9,247	Saturated vapour	689,48	170	-	-	15	0,137
10	0,25240	0,0016	0,0016	-	9	6300	-	-	Air	-	-	-	206,67	15	0,41
11	-	-	-	-	-	15000	-	2,983	-	-	-	-	-	-	0,32
12	-	-	-	-	-	12000	-	0,969	-	-	-	-	-	-	0,24
13	-	-	-	-	-	12000	-	1,491	-	-	-	-	-	-	0,23
14	-	-	-	-	-	1000	-	0,045	-	-	-	-	-	-	0,21
15	-	-	-	-	-	120000	-	1,491	-	-	-	-	-	-	0,49
16	0,30480	0,0008	0,0008	-	45	12000	-	4,4-50	Vapour/exhaust gas	689,48	537,78	0,0191	-	-	0,25
17	0,24765	0,0048	0,0016	-	7	-	-	14,914	-	-	-	-	-	-	-
18	0,40000	-	-	-	26	5400	-	-	-	-	150	-	-	-	-
19	0,25400	-	-	-	-	-	-	74,569	-	-	-	-	-	-	-
20	0,45720	-	-	-	-	-	-	149,138	-	-	-	-	-	-	-
21	1,52400	-	-	-	-	-	-	503,341	-	-	-	-	-	-	-
22	0,24765	-	-	-	25	-	216	82,026	-	-	-	-	-	-	-
23	0,15240	0,0009	0,0012	-	7	1290	17,27	-	-	-	-	-	-	-	-
24	0,15240	-	-	-	-	3000	17,27	-	-	517,11	-	-	-	-	-
25	-	-	-	-	-	9240	-	2,908	Air	723,95	444	-	-	15	-
26	-	-	-	-	-	10200	-	9,694	Air	723,95	-	-	-	15	-
27	0,11430	-	-	-	-	24000	-	0,250	Vapour	1034,2	-	-	-	-	-
28	0,25400	-	-	-	29	18000	-	96,940	-	-	-	-	-	-	-
29	0,07620	-	-	-	15	10500	-	0,153	-	448,16	-	-	-	-	0,31

at the disk wall was refined so as to obtain the y_+ value equal to $1 \div 2$. This is a structural mesh divided into blocks, which contains $400\,000 \div 500\,000$ finite volumes, depending on a turbine model. The calculation grid was also refined in the inlet and outlet regions. Fig. 3 presents images of the calculation area for several turbine models with one, two and four inlet nozzles. Geometrical parameters of particular investigated models are given in Tab. 2.

Thermodynamic parameters assumed for CFD calculations were found from preliminary 1D model calculations, making use of data from literature sources. It is assumed that the considered Tesla turbine models consist of 11 rotating disks (12 flow channels of the interdisk space). The outer diameter of the disk is equal to 10 cm. The nominal operating conditions are for the mass flow rate of 0.13 kg/s and pressure drop from 14.8 bar to 1.9 bar. Solkatherm®SES36S was assumed to be a working medium. The perfect gas model was chosen for the calculations, assuming the individual gas constant and specific heat as average values from the given expansion range. Values of dynamic viscosity and heat conductivity coefficient were assumed in a similar way. Pressure boundary conditions relevant to compressible flow solution were assumed. However, it should be noted that the perfect gas model assumed for the calculations may be a poor approximation of working medium properties, especially for flow velocities close to the sonic velocity. The calculations were carried out for a range of operating conditions (by changing the available pressure drop) for two rotational speeds of the rotor, namely: 18 000 rpm and 9 000 rpm.

Contours of static pressure and velocity for the investigated turbine models 1-3 are presented in Figs. 4, 5

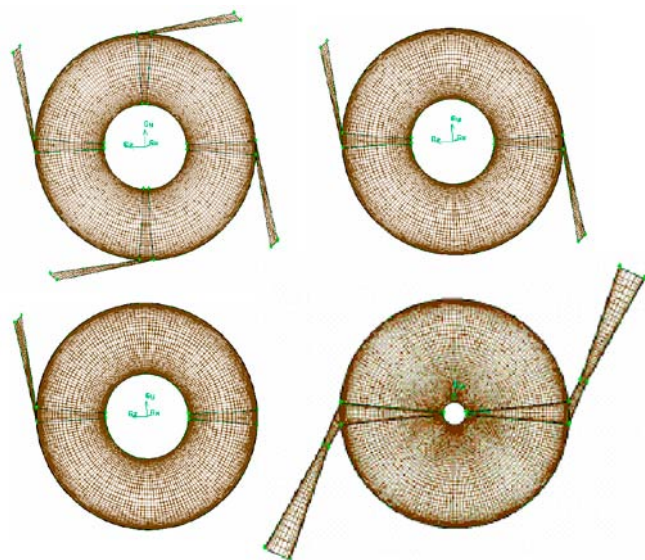


Fig. 3 The calculation domain for four models of the Tesla turbine

Tab. 2 Geometrical parameters of Tesla turbine models

	Model 1	Model 2	Model 3	Model 4
Number of supplying nozzles	1	2	4	2
Outer radius [m]	0.05	0.05	0.05	0.05
Inner radius [m]	0.02	0.02	0.02	0.005
Breadth of gap [m]	0.001	0.0005	0.00025	0.0005
Breadth of inlet [m]	0.003	0.003	0.003	0.008

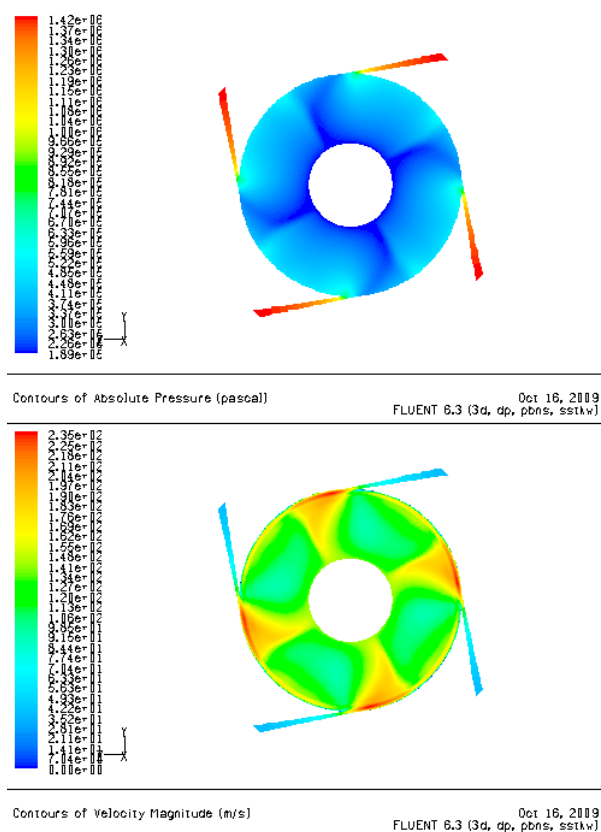


Fig. 4. Contours of static pressure and velocity in flow through the four-nozzle model of the Tesla turbine; $\delta=0.25\text{mm}$, $n=18\,000$, $p_{in}=14.8\text{ bar}$, $T_{in}=410\text{K}$, $G=0.132\text{ kg/s}$, $P=1177\text{ W}$.

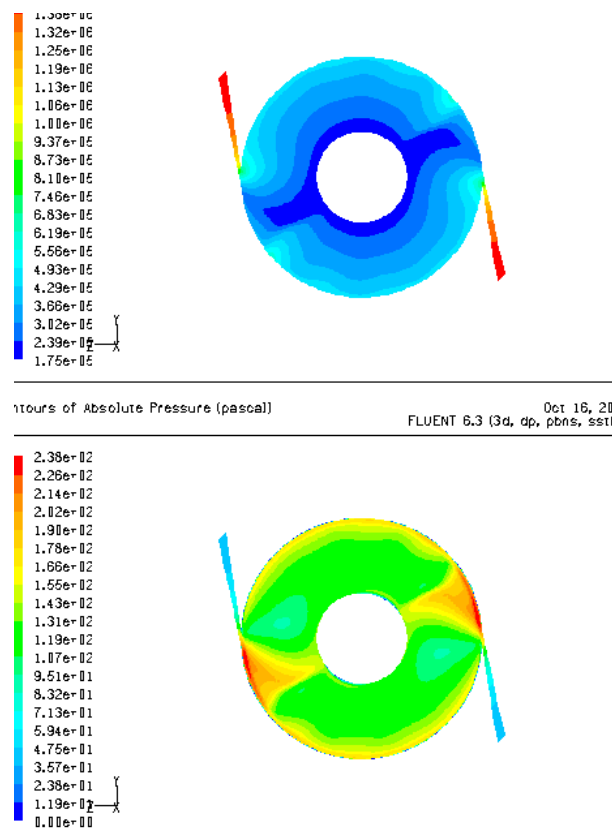


Fig. 5. Contours of static pressure and velocity in flow through the two-nozzle model of the Tesla turbine; $\delta=0.5\text{mm}$, $n=18\,000$, $p_{in}=14.8\text{ bar}$, $T_{in}=410\text{K}$, $G=0.124\text{ kg/s}$, $P=1102\text{ W}$.

and 6. The numbers below the figures show the interdisk gap, rotational speed, inlet pressure and temperature (at the outlet pressure of 1.9 bar) as well as the resultant values – rate of mass flow through 12 interdisk passages and output power generated on both sides of 11 rotating disks. It results from the pressure contours that a part of the available pressure drop is accomplished in the nozzle, the other part takes place in the interdisk space, i.e. in the rotor. In the case of higher loads, configurations of isolines characteristic for the occurrence of shock waves are observed some distance downstream of the inlet nozzle. When a shock wave occurs, an increase of pressure and a decrease of flow velocity takes place. Streamline patterns for the four-nozzle and two-nozzle models operating under part-load conditions (inlet pressure at 7.8 bar) are presented in Fig. 7. It is clear that fluid elements make more than three or four rotations within the interdisk space before they reach the outlet section.

A sample distribution of static pressure and velocity in flow through the model 4 of Tesla turbine (of a small shaft diameter) is presented in Fig. 8. Such a system is characterized by a high reaction, which means that practically the whole pressure drop takes place in the interdisk space of the rotor and that the velocity at the nozzle exit is relatively low. This is due to the vortex motion induced in the interdisk space, which results from the conservation of angular momentum. Thus, flow transition to smaller diameters towards the outlet section causes a velocity increase and a pressure drop. This situation is unfavourable as far as the efficiency is considered – high outlet energy means high flow losses.

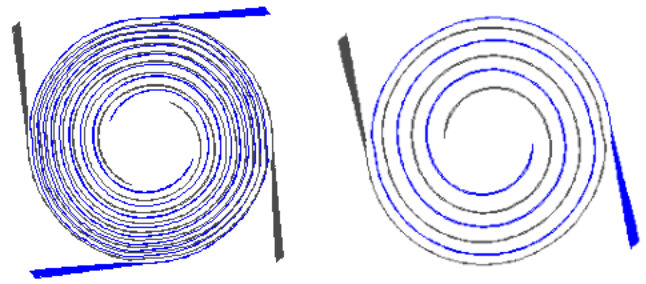


Fig. 7. Streamlines in flow through the four-nozzle and two-nozzle models of the Tesla turbine; $n=18\,000$, $p_{in}=7.8$ bar, $T_{in}=390$ K.

Therefore, the outlet section of a disk turbine should be located at an appropriately large diameter.

The power output, inlet pressure required, flow efficiency and reaction of three investigated models of 11-disk (12-passage) turbine are presented in Figs. 9, 10 and 11 as a function of mass flow rate. The model with four nozzles gives the largest power and flow efficiency. Values of power and efficiency obtained from the two-nozzle model are slightly lower. The respective values for the single-nozzle model are considerably lower. The change in rotational speed from 9000 rpm to 18000 rpm leads to a significant power and efficiency increase. For the rotational speed of $n=18000$ rpm, at the nominal pressure drop from 14.8 to 1.9 bar, which refers to the nominal flow rate of about 0.13 kg/s, the output power of the investigated models of 11-disk turbine amounts to about 1020 W for a single-nozzle model, increasing to 1100 W for the two-nozzle model, to 1180 W for the four-nozzle model. At $n=18000$ rpm, the calculated efficiency

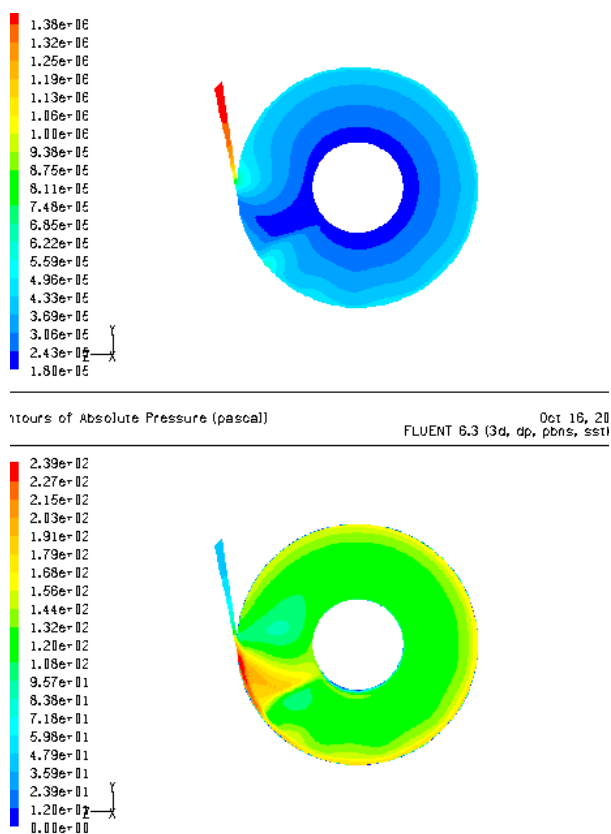


Fig. 6. Contours of static pressure and velocity as well as form of pathlines in flow through Tesla turbine model; $\delta=1$ mm, $n=18\,000$, $p_{in}=10.8$ bar, $T_{in}=390$ K, $G'=0.024$ kg/s, $P'=109.7$ W

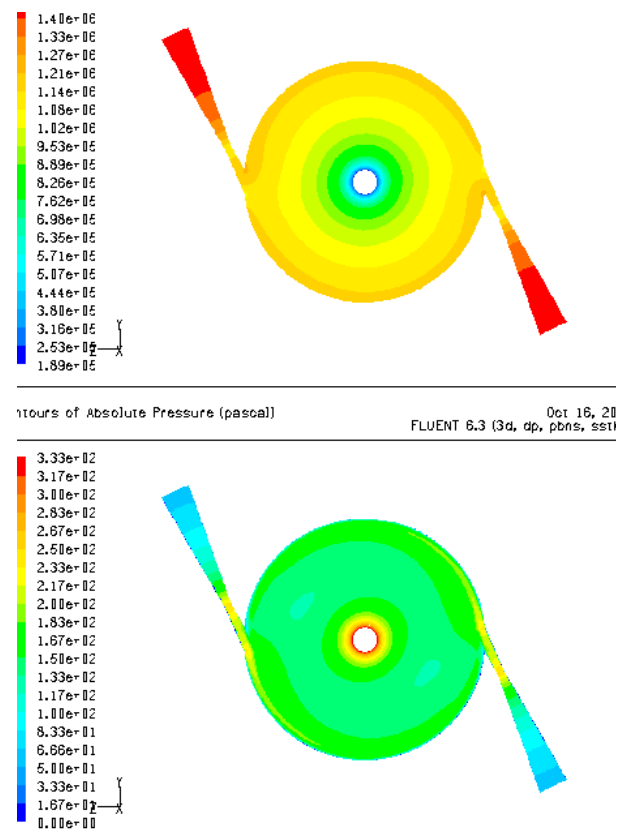


Fig. 8. Contours of static pressure and velocity in flow through the model 4 of the Tesla turbine with a small shaft small diameter; $\delta=0.5$ mm, $n=18\,000$, $p_{in}=14.8$ bar, $T_{in}=410$ K.

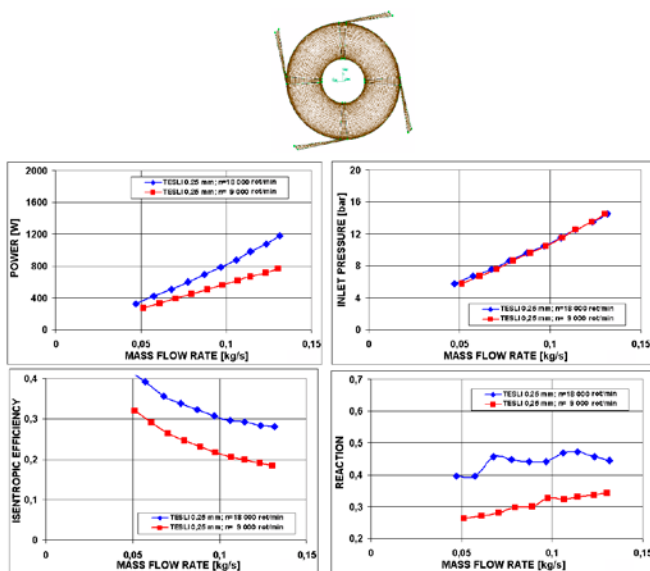


Fig. 9. The power output, inlet pressure, flow efficiency and reaction of an 11-disk turbine as a function of flow rate; the system supplied from four nozzles $\delta=0.25\text{mm}$.

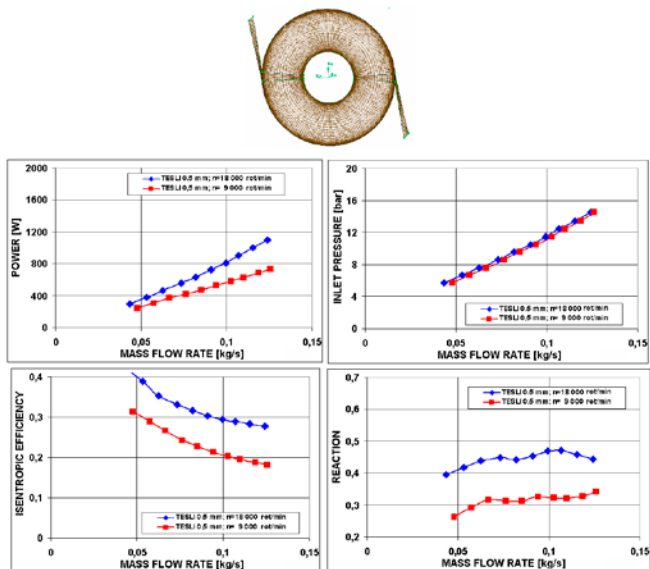


Fig. 10. The power output, inlet pressure, flow efficiency and reaction of an 11-disk turbine as a function of flow rate; the system supplied from two nozzles $\delta=0.5\text{mm}$.

of the models at the nominal operating conditions is equal to 25.5% for the single-nozzle model, increasing to 27% for the two-nozzle model, to 28% for the four-nozzle model. For the rotational speed of $n=9000\text{ rpm}$, at the nominal flow rate of 0.13 kg/s (and nominal pressure drop from 14.8 to 1.9 bar) the output power of the investigated models of 11-disk turbine amounts to about 700 W for a single-nozzle model, increasing to 760 W for the two-nozzle model, to 780 W for the four-nozzle model. At $n=9000\text{ rpm}$, the calculated efficiency of the models at the nominal operating conditions is equal to 17% for the single-nozzle model, increasing to 18.2% for the two-nozzle model, to 18.5% for the four-nozzle model. It is also important to note that for lower loads below nominal operating conditions the flow efficiency is increased. The reaction of the models at $n=18000\text{ rpm}$ varies within the

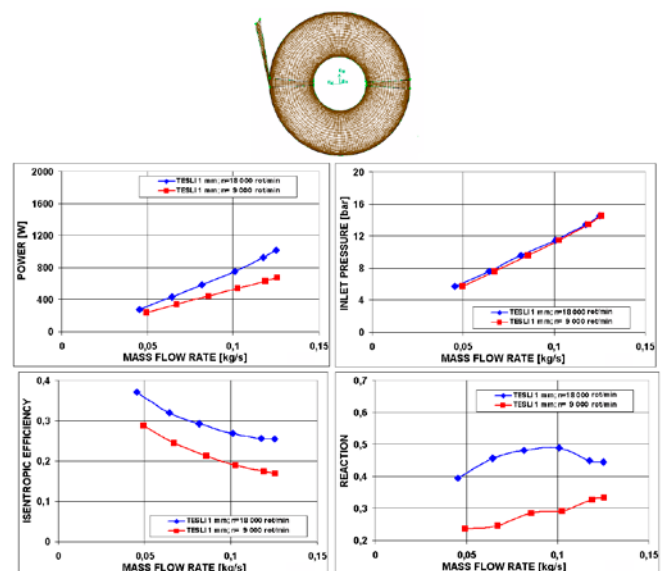


Fig. 11. The power output, inlet pressure, flow efficiency and reaction of an 11-disk turbine as a function of flow rate; the system supplied from one nozzle $\delta=1\text{mm}$.

range of $0.4 \div 0.5$, at $n=9000\text{ rpm}$ changing between $0.25 \div 0.35$. The characteristics of the model no. 4 are here omitted because of a low value of flow efficiency. The internal efficiency of this model is not greater than 10% over the whole range of investigated loads.

Closing remarks and direction of future works

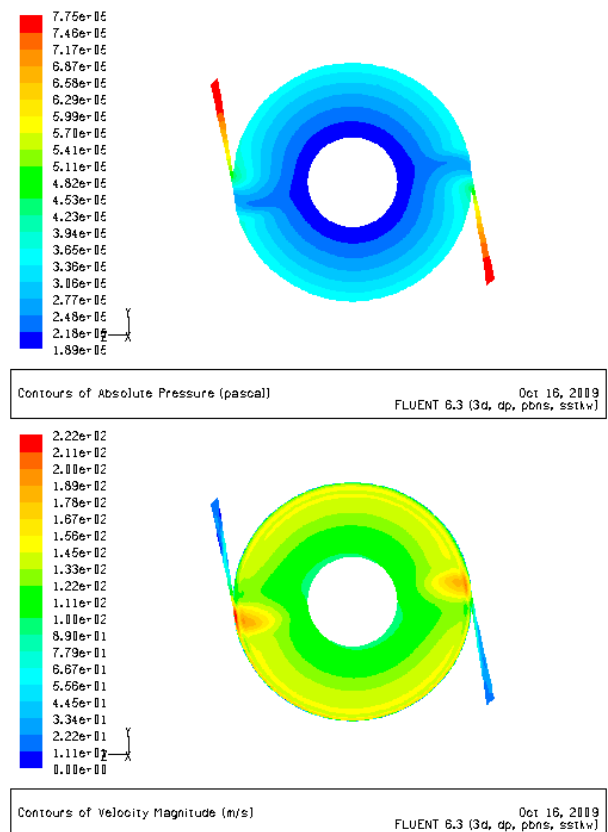


Fig. 12. Contours of static pressure and velocity in flow through the large diameter two-nozzle model of the Tesla turbine; $d=32\text{mm}$, $\delta=0.5\text{mm}$, $n=9000$, $p_{in}=7.8\text{ bar}$, $T_{in}=390\text{K}$, $G=0.119\text{ kg/s}$, $P=1312\text{ W}$

The flow efficiency of the investigated models 1-3 of a Tesla turbine obtained by means of numerical calculations from the code Fluent fall within the range of efficiency values quoted in Introduction based on the literature search. The calculations also highlight some features of operation of the Tesla turbine from a point of view different than that presented in a majority of publications. First of all, the Tesla turbine operates as a reaction turbine with a large pressure drop within the interdisk space. The diameter of the outflow area from the intersdisk space should be still large enough to avoid large outflow velocities. It can also be expected that the lengthening of the friction path within the interdisk space would result in a more effective power transfer.

The above conclusions lead to an idea of increased disk diameter of the Tesla turbine, also accompanied by a decreased cross-section area of the inlet passages. To verify this idea, preliminary calculations were performed for two variants of disk diameter of the two-nozzle model of the Tesla turbine scaled up to 16 cm and 32 cm. In both cases the distance between the disks was equal to 0,5 mm. The supply of medium was accomplished by means of two nozzles located opposite to each other. Sample distributions of pressure and velocity fields in the interdisk space of the Tesla turbine model with the outer diameter equal to 32 cm are shown in Fig. 12, whereas power and efficiency characteristics are displayed in Fig. 13. Within the presented range of mass flow rate (between 0.1 and 0.4 kg/s) and pressure drop (between 7.8 and 14.8 bar) the calculated flow efficiencies oscillate around 50%.

It seems justified to conclude that precise optimization of the Tesla turbine design and geometrical parameters could ensure values of the output power and efficiency similar to those achieved by small bladed turbines. However, the rotational speed of the Tesla turbine rotor is several times lower as compared with small bladed turbines of rotational speed 100 000 rpm. This makes the Tesla turbine an attractive proposal for small heat and power stations, e.g. of heat capacity 20 kW.

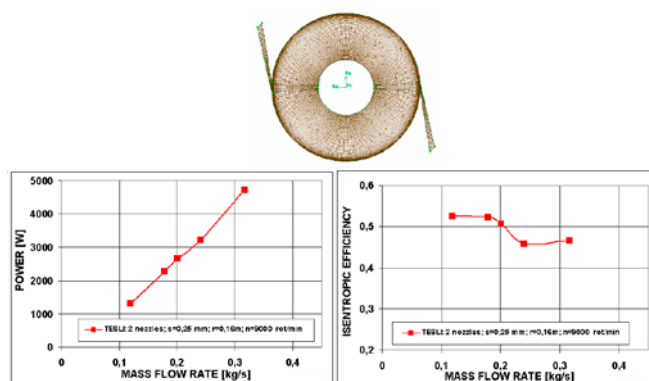


Fig. 13 The power output and efficiency of an 11-disk turbine of a large shaft diameter (32 cm) as a function of flow rate; the system supplied from two nozzles $\delta=0.5\text{mm}$.

Bibliography

1. Beans, W.E.: „Investigation Into the Performance Characteristics of a Friction Turbine”. Journal of Spacecraft, January 1966
2. Cairnes W. M. J.: „The Tesla Disc Turbine”. Camden Miniature Steam Services, 2001
3. Davydov, A. B., and Sherstyuk, A.N.: „Experimental Research on a Disc Microturbine”. Russian Engineering Journal, Issue 8, 1980
4. Gingery V.: „Building the Tesla Turbine”. ISBN 1-878087-29-0, David J. Gingery Publishing, 2004;
5. Gruber, Earl L.: „An Investigation of a Turbine with a Multiple Disc Rotor”. Thesis, Arizona State University, Tempe, Arizona, 1960
6. Ladino F. R.: „Numerical Simulation of the Flow Field in a Friction-Type Turbine (Tesla Turbine)”. Diploma Thesis, Institute of Thermal Powerplants, Vienna University of Technology, 2004
7. North, Richard, C.: „An Investigation of the Tesla Turbine”. Thesis, University of Maryland, 1969;
8. Rice, Warren: „An Analytical and Experimental Investigation of Multiple-Disk Turbines”. Journal of Engineering for Power, Trans. ASME, January 1965
9. Rice, Warren: „Tesla Turbomachinery”. Conference Proceedings of the 4th International Tesla Symposium, Serbian Academy of Sciences and Arts, Belgrade, Yugoslavia, September 22-25, 1991
10. Schmidt D. D.: „Final Report on Biomass Boundary Layer Turbine Power “ Energy Innovations Small Grant, EISG Final Report, Appendix A FAR 00-06, 2002
11. Tesla Nikola: „Turbine”. Patent no: 1,061,206., United States Patent Office, Nikola Tesla, of New York N. Y., Patented May 6, 1913;
12. Fluent Inc.: Fluent/UNS/Rampant „User’s Guide”, 2000
13. Fluent Inc.: Gambit „User’s Guide”. 2000.
14. <http://phoenixnavigation.com/> (Phoenix Navigation & Guidance Inc. Munising, Michigan and Phoenix Turbine Builders Club)